Inorg. Chem. **2008**, *47*, 5616−5624

Ruthenium(II) 2,2′-Bibenzimidazole Complex as a Second-Sphere Receptor for Anions Interaction and Colorimeter

Ying Cui,[†,‡] Yan-Li Niu,[†] Man-Li Cao,[†] Ke Wang,[†] Hao-Jun Mo,[†] Yong-Rui Zhong,[†] and Bao-Hui Ye*[,†]

MOE Laboratory of Bioinorganic and Synthetic Chemistry, School of Chemistry and Chemical Engineering, Sun Yat-Sen University, Guangzhou 510275, China, and Department of Pharmacy, Guangdong Food and Drug Vocational College, Guangzhou 510520, China

Received October 16, 2007

A ruthenium(II) complex $[Ru(bpy)_2(H_2bbim)](PF_6)_2$ (**1**) as anions receptor has been exploited, where Ru(II)-bpy moiety acts as a chromophore and the H_2bbim ligand as an anion binding site. A systematic study suggests that **1** interacts with the Cl^-, Br^-, I^-, NO_3^-, HSO_4^-, and $H_2PO_4^-$ anions via the formation of hydrogen bonds. Whereas **1** undergoes a stepwise process with the addition of F^- and OAc^- anions: formation of the monodeprotonated complex $[Ru(bpy)_2(Hbbim)]$ with a low anion concentration, followed by the double-deprotonated complex $[Ru(bpy)_2(bbim)]$, in the presence of a high anion concentration. These stepwise processes concomitant with the changes of vivid colors from yellow to orange brown and then to violet can be used for probing the F^- and OAc^- anions by naked eye. The deprotonation processes are not only determined by the basicity of the anion but also related to the strength of hydrogen bonding, as well as the stability of the formed compounds. Moreover, a double-deprotonated complex $[Ru(bpy)_2(bbim)] \cdot CH_3OH \cdot H_2O$ (**3**) has been synthesized, and the structural changes induced by the deprotonation has also been investigated. In addition, complexes $[Ru(bpy)_2(Hbbim)]_2(HOAc)_3Cl_2 \cdot 12H_2O$ (**2**), $[Ru(bpy)_2(Hbbim)](HCCl_3CO_2)(CCl_3CO_2) \cdot 2H_2O$ (**4**), and $[Ru(bpy)_2(H_2bbim)](CF_3CO_2)_2 \cdot 4H_2O$ (**5**) have been synthesized to observe the second sphere coordination between the Ru(II)-H_2bbim moiety and carboxylate groups via hydrogen bonds in the solid state.

Introduction

Anion-selected recognition and sensing is of great interest because anions play important roles in chemical, biological, and environmental processes.[1–4] One of the convenient and efficient strategies for the design and construction of a colorimetric sensor for anions is second-sphere coordination, the interaction between already coordinatively saturated metal complexes and external ligands, for example, through hydrogen bonding.[5,6] The Ru(II) polypyridyl complexes with excellent redox and photo properties, particularly, high stability and absorption and emission spectra within the visible range, have been widely employed as chromophores.[7] They have changes of color visible when the second-sphere coordination receptors interact with anions via hydrogen bonds.[8–17]

* To whom correspondence should be addressed. Fax: (86)-20-84112245. Tel: (86)-20-84112469. E-mail: cesybh@mail.sysu.edu.cn (B.-H.Y.).
† Sun Yat-Sen University.
‡ Guangdong Food and Drug Vocational College.

(1) (a) Beer, P. D.; Gale, P. A. *Angew. Chem., Int. Ed.* **2001**, *40*, 486. (b) Sessler, J. L.; Davis, J. M. *Acc. Chem. Res.* **2001**, *34*, 989. (c) Martinez-Manez, R.; Sancenon, F. *Chem. Rev.* **2003**, *103*, 4419. (d) Bowman-James, K. *Acc. Chem. Res.* **2005**, *38*, 671. (e) Amendola, V.; Gómez, E. D.; Fabbrizzi, L.; Licchelli, M. *Acc. Chem. Res.* **2006**, *39*, 343.
(2) Gale, P. A. *Coord. Chem. Rev.* **2003**, *240*, 1–226.
(3) *Anion Receptor Chemistry*; Monographs in Supramolecular Chemistry; Sessler, J. L., Gale, P. A., Cho, W. S., Stoddart, J. F., Ed.; Royal Society of Chemistry: Cambridge, U.K.; 2006.
(4) Gale, P. A. *Coord. Chem. Rev.* **2006**, *250*, 2917–3244.
(5) Loeb, S. J. In *Comprehensive Supramolecular Chemistry*; Lehn, J.-M., Atwood, J. L., Davies, J. E. D., McNichol, D. D.; Vögtle, F.; Gokel, G. W., Ed.; Pergamon: Oxford, U.K., 1996; Vol. 1, pp. 733−753.
(6) Balzani, V.; Sabbatini, N.; Scandola, F. *Chem. Rev.* **1986**, *86*, 319.
(7) (a) Balzani, V.; Juris, A.; Venturi, M. *Chem. Rev.* **1996**, *96*, 759. (b) de Silva, A. P.; Guarantne, H. Q.; Gunnlaugsson, N. T.; Huxley, A. J.; McCoy, C. P.; Rademacher, J. T.; Rice, T. R. *Chem. Rev.* **1997**, *97*, 1515. (c) Schubert, U. S.; Eschbaumer, C. *Angew. Chem., Int. Ed.* **2002**, *41*, 2893. (d) Browne, W. R.; Hage, R.; Vos, J. G. *Coord. Chem. Rev.* **2006**, *250*, 1653. (e) Medlycott, E. A.; Hanan, G. S. *Coord. Chem. Rev.* **2006**, *250*, 1763.
(8) Rice, C. R. *Coord. Chem. Rev.* **2006**, *250*, 3190.
(9) (a) Beer, P. D.; Hayes, E. J. *Coord. Chem. Rev.* **2003**, *240*, 167. (d) Beer, P. D.; Bayly, S. R. *Top. Curr. Chem.* **2005**, *255*, 125.
(10) Watanabe, S.; Onogawa, O.; Komatsu, Y.; Yoshida, K. *J. Am. Chem. Soc.* **1998**, *120*, 229.

10.1021/ic702050b CCC: $40.75
Published on Web 05/23/2008

Recently, we and others have applied the strategy of second-sphere coordination to design ionic receptors based on the 2,2′-biimidazole (H_2biim) complexes.[18–22] The most interesting and important feature for such construction is that the chelating coordination enforces the syn conformation and then engages in hydrogen bonding via the externally directed pair of N−H groups of the H_2biim ligand. The complex $[Ru(bpy)_2(H_2biim)](PF_6)_2$ (bpy = 2,2'-bipyridine) donates protons for hydrogen bonds to Cl^-, Br^-, I^-, NO_3^-, HSO_4^-, $H_2PO_4^-$, OAc^-, and F^- anions and turns from yellow to orange brown and then to violet because of the second-sphere donor−acceptor interactions between Ru(II)-H_2biim and anions. This process outputs vivid colors that can be distinguished by naked eye.[18] As part of an ongoing study, we extend the insight into the 2,2'-bibenzimidazole (H_2bbim) ligand. Compared with the H_2biim ligand, the side-by-side steric repulsion between the H_8 of the H_2bbim ligands (see Scheme S1 in the Supporting Information) should effectively prevent the self-aggregation via complementary hydrogen bonds, which have been widely observed in H_2biim complexes in solution[18,22] and in crystal engineering (where each H_2biim ligand is a monodeprotonated, anionic imidazolate ring).[23–25] Such self-aggregation perturbs the interaction of H_2biim complexes with anions via hydrogen bonding.[23b] On the other hand, the pK_a values of Ru(II)-H_2bbim (pK_{a1} = 5.7 and pK_{a2} = 10.1) are much lower than those of Ru(II)-H_2biim (pK_{a1} = 7.2 and pK_{a2} = 12),[26,27] indicating that the former may be easy to donate proton to anion. The spectroscopic and electrochemical properties of Ru(II)-H_2bbim have been well investigated in solution.[26–28] Although H_2bbim complexes have been found, formation of hydrogen bonds with the external anions, such as halide,[29] perchlorate,[29a] and carboxylate[30] in the solid state, a systematic insight into the interaction of H_2biim or H_2bbim complex as an anionic receptor in solution is rare.[18–22] We report herein a second-sphere coordination receptor $[Ru(bpy)_2(H_2bbim)](PF_6)_2$ (**1**) for anions such as Cl^-, Br^-, I^-, NO_3^-, HSO_4^-, $H_2PO_4^-$, OAc^-, and F^-. Where Ru(II)-bpy moiety being a characteristic in absorption and emission spectra within the visible range acts as a chromophore, and the H_2bbim ligand has a bifunctionality, the imino moieties can be coordinated to a Ru(II)-bpy fragment as a first coordination sphere and the amino groups as a second-sphere coordination may donate 2-fold hydrogen bonds to anions (Scheme 1). It displays vivid colors when the binding event takes place on the second sphere. To observe the second-sphere coordination between the Ru(II)-H_2bbim moiety and carboxylate groups via hydrogen bonds in the solid state, complexes $[Ru(bpy)_2(Hbbim)]_2(HOAc)_3Cl_2\cdot 12H_2O$ (**2**), $[Ru(bpy)_2(Hbbim)](HCCl_3CO_2)(CCl_3CO_2)\cdot 2H_2O$ (**4**), and $[Ru(bpy)_2(H_2bbim)](CF_3CO_2)_2\cdot 4H_2O$ (**5**) have been synthesized. In addition, a double-deprotonated complex $[Ru(bpy)_2(bbim)]\cdot CH_3OH\cdot H_2O$ (**3**) has been synthesized, and the structural changes induced by deprotonation has also been discussed.

Scheme 1. Schematic Representation of the First (Yellow) and the Second Coordination Sphere (Gray) for Complex **1**

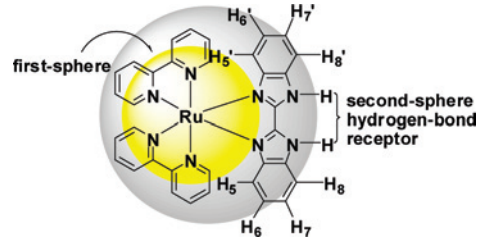

Experimental Section

Materials and Methods. The reagents and solvents employed were commercially available and were used as received without further purification. The C, H, and N microanalyses were carried out with a Vario EL elemental analyzer. The FT-IR spectra were recorded from KBr pellets in the range of 400−4000 cm^{-1} on a Bruker TENSOR 27 FT-IR spectrometer. ^1H NMR spectra were recorded on a Varian Mercury-Plus 300 NMR spectrometer with chemical shifts (in ppm) relative to tetramethylsilane (TMS). Electron spray ionization (ESI) mass spectra were obtained on a LCQ DECA XP quadrupole ion trap mass spectrometer with MeCN as the carrier solvent. Thermogravimetric data were collected on a Netzsch TG-209 analyzer in nitrogen at a heating rate of 10 °C

(11) Deetz, M. J.; Smith, B. D. *Tetrahedron Lett.* **1998**, *39*, 6841.
(12) Aoki, S.; Zulkefeli, M.; Shiro, M.; Kohsako, M.; Takeda, K.; Kimura, E. *J. Am. Chem. Soc.* **2005**, *127*, 9129.
(13) Anzenbacher, P., Jr.; Tyson, D. S.; Jursikova, K.; Castellano, F. N. *J. Am. Chem. Soc.* **2002**, *124*, 6232.
(14) Mizuno, T.; Wei, W.-H.; Eller, L. R.; Sessler, J. L. *J. Am. Chem. Soc.* **2002**, *124*, 1134.
(15) Lazarides, T.; Miller, T. A.; Jeffery, J. C.; Ronson, T. K.; Adams, H.; Ward, M. D. *Dalton Trans.* **2005**, 528.
(16) (a) Lin, Z.-H.; Ou, S.-J.; Duan, C.-Y.; Zhang, B.-G.; Bai, Z.-P. *Chem. Commun.* **2006**, 624. (b) Lin, Z.-H.; Zhao, Y.-G.; Duan, C.-Y.; Zhang, B.-G.; Bai, Z.-P. *Dalton Trans.* **2006**, 3678.
(17) Jose, D. A.; Kar, P.; Koley, D.; Ganguly, B.; Thiel, W.; Ghosh, H. N.; Das, A. *Inorg. Chem.* **2007**, *46*, 5576.
(18) Cui, Y.; Mo, H.-J.; Chen, J.-C.; Niu, Y.-L.; Zhong, Y.-R.; Zheng, K.-C.; Ye, B.-H. *Inorg. Chem.* **2007**, *46*, 6427.
(19) Rau, S.; Buttner, T.; Temme, C.; Ruben, M.; Gorls, H.; Walther, D.; Duati, M.; Fanni, S.; Vos, J. G. *Inorg. Chem.* **2000**, *39*, 1621.
(20) (a) Fortin, S.; Beauchamp, A. L. *Inorg. Chem.* **2001**, *40*, 105. (b) Fortin, S.; Fabre, P.-L.; Dartiguenave, M.; Beauchamp, A. L. *J. Chem. Soc., Dalton Trans.* **2001**, 3520.
(21) Ion, L.; Morales, D.; Perez, J.; Riera, L.; Riera, V.; Kowenicki, R. A.; McPartlin, M. *Chem. Commun.* **2006**, 91.
(22) Derossi, S.; Adams, H.; Ward, M. D. *Dalton Trans.* **2007**, 33.
(23) (a) Tadokoro, M.; Nakasuji, K. *Coord. Chem. Rev.* **2000**, *98*, 205. (b) Tadokoro, M.; Kanno, H.; Kitajima, T.; Shimada-Umemoto, H.; Nakanishi, N.; Isobe, K.; Nakasuji, K. *Proc. Nat. Acad. Sci. U.S.A.* **2002**, *99*, 4950.
(24) Öhrström, L.; Larsson, K. *Dalton Trans.* **2004**, 347.
(25) Gruia, L. M.; Rochon, F. D.; Beauchamp, A. L. *Can. J. Chem.* **2006**, *84*, 949.
(26) Haga, M.-A. *Inorg. Chim. Acta* **1983**, *75*, 29.
(27) Rillema, D. P.; Sahai, R.; Matthews, P.; Edwards, A. K.; Shaver, R. J.; Morgan, L. *Inorg. Chem.* **1990**, *29*, 167.
(28) Yin, J.; Elsenbaumer, R. L. *Inorg. Chem.* **2007**, *46*, 6891.
(29) (a) Boinnard, D.; Cassoux, P.; Petrouleas, V.; Savariault, J.-M.; Tuchagues, J.-P. *Inorg. Chem.* **1990**, *29*, 4114. (b) de Lemos, S.; Bessler, K. E.; Lang, E. S. *Z. Anorg. Allg. Chem.* **1998**, *624*, 701. (c) Akutagawa, T.; Hasegawa, T.; Nakamura, T.; Saito, G. *CrystEngComm* **2003**, *5*, 54.
(30) (a) Rau, S.; Böttcher, L.; Schebesta, S.; Stollenz, M.; Görls, H.; Walther, D. *Eur. J. Inorg. Chem.* **2002**, 2800. (b) Wen, L.; Li, Y.; Dang, D.; Tian, Z.; Ni, Z.; Meng, Q. *J. Solid State Chem.* **2005**, *178*, 3336. (c) Xia, C.-K.; Lu, C.-Z.; Yuan, D.-Q.; Zhang, Q.-Z.; Wu, X.-Y.; Xiang, S.-C.; Zhang, J.-J.; Wu, D.-M. *CrystEngComm* **2006**, *8*, 281.

Table 1. Crystal Data and Structure Refinement for Complexes **2**−**4**

	2	**3**	**4**
formula	$C_{74}H_{86}N_{16}O_{18}Cl_2Ru_2$	$C_{35}H_{30}N_8O_2Ru$	$C_{38}H_{30}N_8O_6Cl_6Ru$
fw	1759.44	695.74	1008.46
cryst syst	triclinic	monoclinic	triclinic
space group	$P\bar{1}$	Pc	$P\bar{1}$
a (Å)	13.687(1)	9.696(1)	9.904(1)
b (Å)	15.555(1)	9.480(1)	11.735(1)
c (Å)	19.550(1)	18.326(1)	18.913(2)
α (deg)	86.562(1)	90	88.102(2)
β (deg)	76.866(1)	115.17(3)	74.916(2)
γ (deg)	75.104(1)	90	75.501(2)
V (Å^3)	3917.1(5)	1524.6(2)	2053.1(4)
D_c (g cm^{-3})	1.472	1.516	1.631
Z	2	2	2
μ (mm^{-1})	0.532	0.562	0.830
data/restraints/params	15 206/0/1004	5463/2/415	7805/0/541
GOF on F^2	1.01	0.980	1.01
R1 [$I > 2\sigma(I)$], wR2 (all data)[a]	0.0804, 0.2200	0.0350, 0.0781	0.0515, 0.1278
$\Delta\rho_{max}/\Delta\rho_{min}$ (e Å^{-3})	1.27/−1.25	0.87/-0.34	0.91/−0.57

[a] $R1 = \sum||F_o|-|F_c||/\sum|F_o|$, $wR2 = [\sum w(F_o^2 - F_c^2)^2/\sum w(F_o^2)^2]^{1/2}$.

min^{-1}. *cis*-[Ru(bpy)$_2$Cl$_2$]·2H$_2$O, [Ru(bpy)$_2$(H$_2$bbim)]Cl$_2$, and H$_2$bbim were synthesized as reported in the literature procedures.[31−33]

Synthesis of [Ru(bpy)$_2$(H$_2$bbim)](PF$_6$)$_2$ (1). The title complex was synthesized in accordance with the published procedure.[33] Yield: 81%. ^{1}H NMR (DMSO-d_6): δ 14.38 (b, 2H, N−H), 8.84 (d, J = 7.9 Hz, 2H, bpy), 8.74 (d, J = 7.9 Hz, 2H, bpy), 8.21 (t, 2H, bpy), 8.04 (t, 2H, bpy), 7.98 (d, J = 5.5 Hz, 2H, bpy), 7.86 (d, J = 5.5 Hz, 2H, bpy), 7.83 (d, J = 11.0 Hz, 2H, H$_8$), 7.58 (t, 2H, bpy), 7.46 (t, 2H, bpy), 7.34 (t, 2H, H$_7$), 7.02 (t, 2H, H$_6$), 5.60 (d, J = 8.2 Hz, 2H, H$_5$). ESI-MS: m/z = 647.1 [M − 2PF$_6$ − H]$^+$, 324.1 [M − 2PF$_6$]$^{2+}$. FT-IR data (cm^{-1}): 3435 br, 1614 m, 1456 m, 1419 m, 1351 m, 1034 m, 843 vs, 757 s, 557 s.

Synthesis of [Ru(bpy)$_2$(Hbbim)]$_2$(HOAc)$_3$Cl$_2$·12H$_2$O (2). Sodium acetate (0.1 mmol) was added to a solution of [Ru(bpy)$_2$(H$_2$bbim)]Cl$_2$ (72 mg, 0.1 mmol) in methanol/acetonitrile (40 mL). The mixture was stirred at room temperature for 2 h, then, filtered. The filtrate was kept at room temperature to volatilize the solvent. After several days, the red crystals of **2** were obtained in yield of 56%. $C_{74}H_{86}N_{16}O_{18}Cl_2Ru_2$ (1759): C 50.48, H 4.89, N 12.73; found C 50.39, H 4.82, N 12.42. FT-IR data (cm^{-1}): 3419 br, 1598 s, 1545 s, 1416 vs, 1257 m, 746 s. The TGA experiment of **2** was carried out from 20 to 400 °C. The weight loss of 17.0% in the range of 20−260 °C (see Figure S1 in the Supporting Information) corresponds to the loss of 12 water molecules and one acetic acid molecule (calculated 15.9%).

Synthesis of [Ru(bpy)$_2$(bbim)]·CH$_3$OH·H$_2$O (3). NaOH solution (1 M, 0.15 mmol) was added to the solution of [Ru(bpy)$_2$(H$_2$bbim)]Cl$_2$ (0.05 mmol, 36 mg) in methanol/acetonitrile (25 mL). The mixture solution was stirred at room temperature for 2 h and then filtered. The filtrate was kept at room temperature to volatilize the solvent. After several days, deep red crystals of **3** were obtained. Yield: 60%. $C_{35}H_{30}N_8O_2Ru$ (695): C 60.43, H 4.32, N 16.11; found C 59.82, H 4.52, N 15.76. ^{1}H NMR (DMSO-d_6): δ 8.73 (d, J = 8.0 Hz, 2H, bpy), 8.63 (d, J = 8.0 Hz, 2H, bpy), 8.07 (t, 2H, bpy), 7.92(d, J = 5.5 Hz, 2H, bpy), 7.85 (t, 2H, bpy), 7.71 (d, J = 5.8 Hz, 2H, bpy), 7.48 (t, 2H, bpy), 7.40 (d, J = 7.7 Hz, 2H, H$_8$), 7.36 (t, 2H, bpy), 6.73 (t, 2H, H$_7$), 6.44 (t, 2H, H$_6$), 5.34 (d, J = 7.8 Hz, 2H, H$_5$). FT-IR data (cm^{-1}): 3439 br, 2923 s, 2854 s, 1601 s, 1456 m, 1345 s, 1288 m, 1114 m, 1026 s, 750 vs, 653 m.

Synthesis of [Ru(bpy)$_2$(Hbbim)](HCCl$_3$CO$_2$)(CCl$_3$CO$_2$)·2H$_2$O (4) and [Ru(bpy)$_2$(H$_2$bbim)](CF$_3$CO$_2$)$_2$·4H$_2$O (5). The title complexes were synthesized as the procedure of **2**, but trichloroacetic acid/NaOH or triflluoroacetic acid/NaOH was used in place of sodium acetate. The red crystals of **4** and **5** were obtained in yields of 80% and 46%, respectively. FT-IR data for **4** (cm^{-1}): 3432 br, 3060 m, 2924 m, 1601 s, 1458 s, 1348 vs, 1287 s, 1157 m, 1011 m, 749 vs, 653 m. $C_{38}H_{34}N_8O_8F_6Ru$ (945): C 48.25, H 3.59, N 11.85; found C 48.44, H 3.72, N 12.13. FT-IR data for **5** (cm^{-1}): 3434 br, 3071 m, 2925 m, 1686 vs, 1416 m, 1353 m, 1198 vs, 1130 vs, 826 m, 762 s, 600 m.

X-ray Crystallography. Diffraction intensities for **2** were collected at 152 K, and **3** and **4** were collected at 293 K on a Bruker Smart Apex CCD diffractometer with graphite-monochromated Mo Kα radiation (λ = 0.71073 Å). Absorption corrections were applied using SADABS.[34] The structures were solved by Patterson methods and refined with the full-matrix least-squares technique using SHELXS-97 and SHELXL-97 programs, respectively.[35] Anisotropic thermal parameters were applied to all non-hydrogen atoms. The organic hydrogen atoms were generated geometrically (C−H = 0.96 Å and N−H = 0.86 Å). The hydrogen atoms of the water molecules were located from difference maps and refined with isotropic temperature factors. Crystal data as well as details of data collection and refinement for the complexes are summarized in Table 1. Selected bond distances and bond angles are listed in Table 2.

General Spectroscopic Methods. Solvent MeCN used for spectral experiments was distilled from CaH$_2$ and kept over 4 Å molecular sieves. Tetrabutylammonium (TBA) salts of F$^-$, Cl$^-$, Br$^-$, I$^-$, NO$_3^-$, HSO$_4^-$, H$_2$PO$_4^-$, and OAc$^-$ were purchased from Alfa Aesar and dissolved in MeCN. Binding constants were performed in duplicate, and the average is reported. All data were manipulated by using the OriginLab software package.

Absorption Spectroscopy. UV−vis spectra were performed on a Shimadzu UV-315 UV−vis spectrophotometer at room temperature. Quartz cuvettes with a 1 cm path length and a 3 mL volume were used for all measurements. For a typical titration experiment, 3 μL aliquots of a TBA salt (5×10^{-3} M in MeCN) were added to a 3 mL solution of **1** in MeCN by a syringe.

(31) Sprintschnik, G.; Sprintschnik, H. W.; Kirsch, P. P.; Whitten, D. G. *J. Am. Chem. Soc.* **1977**, *99*, 4947.
(32) Muller, E.; Bernardinelli, G.; Reedijk, J. *Inorg. Chem.* **1995**, *34*, 5979.
(33) Dose, E. V.; Wilson, L. J. *Inorg. Chem.* **1978**, *17*, 2660.
(34) Sheldrick, G. M. *SADABS, Program for Empirical Absorption Correction of Area Detector Data*; University of Göttingen: Göttingen, Germany, 1996.
(35) Sheldrick, G. M. *SHELXS-97, Program for Crystal Structure Solution and Refinement*; University of Göttingen:Göttingen, Germany, 1997.

Table 2. Selected Bond Lengths (Å) and Angles (deg) of **2**−**4**[a]

complex	2	3	4
Ru−N1	2.064(6)	2.047(3)	2.050(4)
Ru−N2	2.050(5)	2.032(3)	2.040(4)
Ru−N3	2.046(6)	2.042(2)	2.045(4)
Ru−N4	2.042(5)	2.043(2)	2.054(4)
Ru−N5	2.103(5)	2.087(3)	2.094(4)
Ru−N6	2.092(5)	2.084(4)	2.103(4)
C27−C28	1.451(8)	1.450(4)	1.429(7)
C27−N5	1.339(8)	1.353(4)	1.322(5)
C27−N7	1.348(9)	1.341(4)	1.360(6)
C28−N6	1.315(8)	1.356(4)	1.331(6)
C28−N8	1.349(9)	1.336(5)	1.343(6)
N1−Ru−N2	78.9(2)	79.0(1)	79.0(1)
N3−Ru−N4	79.7(2)	78.9(1)	78.6(1)
N5−Ru−N6	78.0(2)	77.4(1)	77.8(1)
N1−Ru−N3	173.8(2)	98.7(1)	97.5(1)
N1−Ru−N4	97.9(2)	176.4(1)	174.9(1)
N1−Ru−N5	93.3(2)	96.4(1)	96.4(1)
N1−Ru−N6	89.5(2)	89.5(1)	89.0(1)
N2−Ru−N3	95.3(2)	87.8(1)	91.0(1)
N2−Ru−N4	91.3(2)	98.2(1)	97.7(1)
N2−Ru−N5	171.4(2)	173.5(1)	172.6(1)
N2−Ru−N6	98.1(2)	97.9(1)	96.2(1)
N3−Ru−N5	92.6(2)	97.5(1)	95.3(1)
N3−Ru−N6	93.7(2)	170.8(1)	171.1(1)
N4−Ru−N5	93.5(2)	87.11)	87.3(1)
N4−Ru−N6	169.0(2)	93.2(1)	95.3(1)
N5−C27−N7	113.0(6)	116.5(3)	113.8(4)
N6−C28−N8	115.8(6)	116.4(3)	112.7(4)
C21−N5−C27	104.9(5)	103.8(3)	105.7(4)
C28−N6−C34	105.1(5)	103.9(3)	105.8(3)
C26−N7−C27	106.9(5)	102.5(3)	105.3(3)
C28−N8−C29	104.6(5)	102.9(3)	107.3(4)
N7−C26−C21	106.4(6)	109.7(3)	107.4(4)
N8−C29−C34	107.1(6)	109.2(3)	106.0(4)

[a] Symmetry code: a $-x, -y, -2-z$; b $1/2-x, -1/2-y, z$.

Table 3. Selected Hydrogen Bonding Lengths (Å) and Bond (deg) of **2**−**4**[a]

D-H···A	D−H	H···A	D···A	∠D−H···A
		2		
N7−H7B···O1A	0.88	1.76	2.640(7)	174
O2A−H···N8	0.70	1.98	2.679(6)	174
O4A−H···N16	0.75	1.94	2.693(7)	175
N15−H15B···O3A	0.88	1.77	2.643(6)	174
		3		
O1w−H1···N8	0.87	2.08	2.979(7)	178
O1−H1B···N7	0.79	2.02	2.805(6)	175
O1w−H2···O1	0.87	2.08	2.926(5)	163
		4		
O3A−H···N7	0.87	1.76	2.630(5)	170
N8−H8B···O4A	0.86	1.93	2.784(5)	173

[a] D, donor atom; A, acceptor atom. Symmetry code: **2** a $x, -1+y, z$; **4** a $1-x, 1-y, -z$.

^{1}H NMR Titration. ^{1}H NMR spectra were recorded on a Varian Mercury-Plus 300 NMR spectrometer with DMSO-d_6 as a solvent and TMS as an internal standard. For the OAc^- anion titration, 22.5 μL aliquots of a $[Bu_4N]OAc$ (0.05 M in DMSO-d_6) were added to a DMSO-d_6 solution of **1** (7.5×10^{-3} M). For the F^- anion, 15 μL aliquots of a $[Bu_4N]F$ (0.075 M in DMSO-d_6) were added to a DMSO-d_6 solution of **1** (7.5×10^{-3} M).

Results and Discussion

Receptor for Cl^-, Br^-, I^-, NO_3^-, HSO_4^-, and $H_2PO_4^-$ Anions. To extend the design and construction strategy of second-sphere receptor for anions, a functional complex **1** was used as a receptor to investigate the interactions with the various anions in solution through spectrophotometric experiments. When 5 equiv of I^- anion in MeCN was added to a 2.5×10^{-5} M solution of **1** in MeCN, as shown in Figure 1, the absorption peak at 465 nm that was assigned to metal−ligand charge transition (MLCT) from Ru(II) to bpy ligand[26–28] did not shift concomitant with the intensity decrease, indicating that the interaction was weak. Moreover, when 5 equiv of Cl^-, Br^-, NO_3^-, and HSO_4^- anions were added to a solution of **1**, the peak at 465 nm shifted to 472 nm, and precipitation appeared when 1 equiv of $H_2PO_4^-$ anion was introduced. The absorption spectral changes are ascribed to the formation of initial hydrogen bonds between H_2bbim N−H groups and the anions.

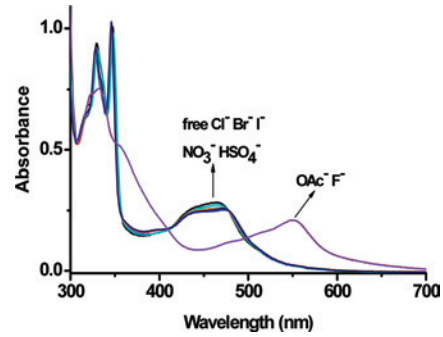

Figure 1. UV−vis spectra of **1** in MeCN solution (2.5×10^{-5} M, black) and the addition of 5 equiv of Cl^- (navy), Br^- (green), I^- (cyan), NO_3^- (orange), HSO_4^- (blue), OAc^- (red), and F^- (violet) anions.

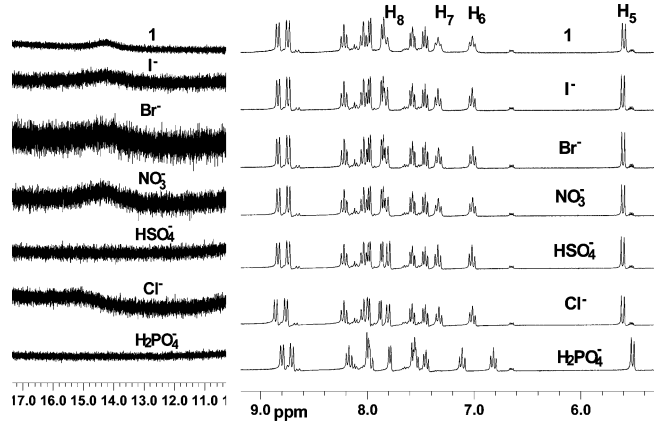

Figure 2. ^{1}H NMR spectra of **1** (7.5×10^{-3} M) in DMSO-d_6 in the absence and presence of 1 equiv of anions.

To further confirm the interactions of **1** and the anions via hydrogen bonding, ^{1}H NMR experiments were carried out in DMSO-d_6 solution. As shown in Figure 2, a singlet at δ 14.38 ppm that was assigned to the two N−H groups of Ru(II)-H_2bbim broadened upon addition of 1 equiv of TBA iodide, bromide, and nitrate to the solution of **1**. However, when 1 equiv of Bu_4NCl was added to the solution of **1**, the N−H signal shifted to 15.10 ppm, indicating that the interaction of **1** and the Cl^- anion is strong. When an equimolar amount of $[Bu_4N]H_2PO_4$ was introduced to the solution of **1**, the N−H signal finally disappeared. Instead, the C−H signals of H_5, H_6 H_7, and H_8 in the phenyl ring displayed markedly upfield shifts, indicating a strong hydrogen bonded interaction between **1** and $H_2PO_4^-$ anion.

Interactions with OAc^- and F^- Anions. As shown in Figure 1, when 5 equiv of OAc^- or F^- anion in MeCN was

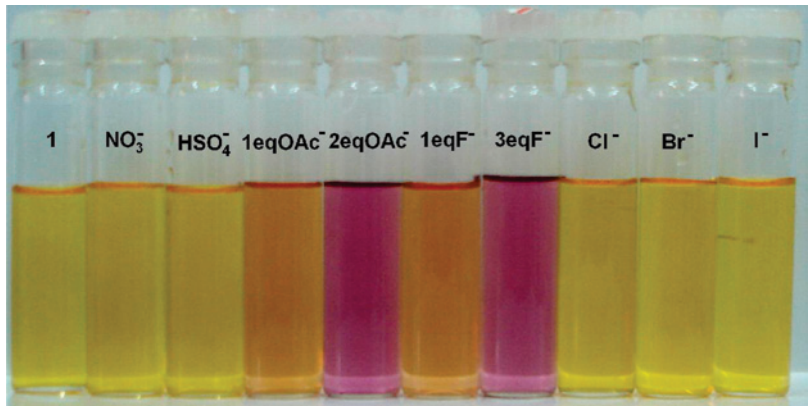

Figure 3. Color changes observed for **1** (8×10^{-5} M) in MeCN solution and in the presence of the corresponding anions as TBA salts.

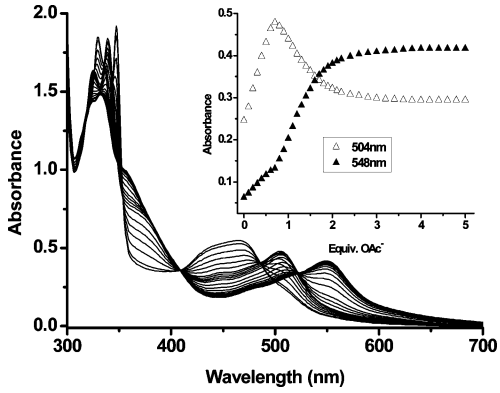

Figure 4. UV−vis titration of **1** in MeCN solution (5×10^{-5} M) upon addition of Bu_4NOAc (0−5 equiv). Insert: Absorbances at 504 and 548 nm versus equivalent of OAc^- anion.

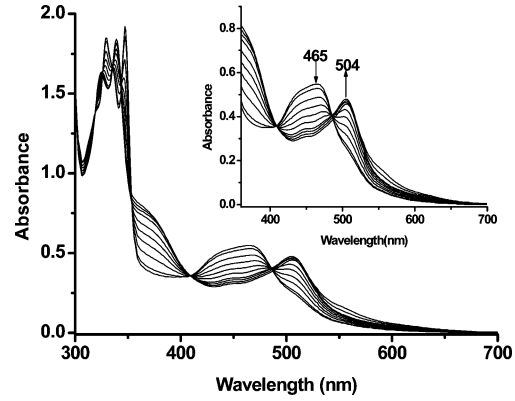

Figure 5. UV−vis titration of **1** in MeCN solution (5×10^{-5} M) upon addition of 0−1 equiv of Bu_4NOAc. Insert: Absorption spectra in the range of 360−700 nm.

added to the solution of **1**, the band at 465 nm was markedly red-shifted to 548 nm, and the yellow, original solution of **1** turned violet, as shown in the picture in Figure 3. The red-shift of the MLCT band can be attributed to the "second-sphere donor−acceptor" interaction between the Ru(II)-H_2bbim and anions.[6,36] Such interaction (monodeprotonation or double-deprotonation in H_2bbim ligand, vide infra) greatly increases the electron density at the Ru(II) center and shifts its oxidation potential to a less-positive value, resulting in the decrease of the MLCT band energy.

To clarify the binding property of **1** toward OAc^- anion, titration experiments were carried out. Figure 4 exhibits the complete family of spectra displacement and the absorption intensity variety of the bands at 504 (first increasing and then decreasing) and 548 nm (increasing) during the titration of a 5×10^{-5} M solution of **1** in MeCN with $[Bu_4N]OAc$. The addition of OAc^- anion induces that the peak at 465 nm gradually decreases, and a new absorption band at 504 nm develops, with color turning from yellow to orange brown (see Figure 3), which reaches its limiting value when 1 equiv of OAc^- anion is added. Continuous addition of OAc^- up to 2 equiv induces that the peak at 504 nm decreases, and a new absorption band at 548 nm progressively develops. The color of the final solution turns to violet. After that, the change of absorption spectra is negligible.

The stepwise changes of the absorption spectra in the titration experiment indicate that the interaction may involve two-step processes. First, from the start to 1 equiv of OAc^- anion addition to the solution of **1**, the new band at 504 nm reached its limiting value, and the color of solution turned from yellow to orange brown. To identify the new species with a characteristic band at 504 nm, 1 equiv of NaOH was added to the solution of **1** to generate the monodeprotonated species $[Ru(bpy)_2(Hbbim)]^+$. Their absorption and ^1H NMR spectra match well (see Figures S2 and S3 in the Supporting Information), demonstrating that a monodeprotonation process takes place upon addition of one equivalent of OAc^-.[26–28] The appearance of two isosbestic points at 318 and 409 nm in the titration profile indicates that the binding of OAc^- to **1** is a clear equilibrium process (Figure 5). The profile of the absorbance at 504 nm (increasing) demonstrates a 1:1 stoichiometry for the receptor−OAc^- interaction. With reference to the spectroscopic observations of the related Ru−H_2biim compounds,[18,21] it is likely that the change in the absorption spectra is a consequence of the formation of an initial hydrogen bonding between the H_2bbim N−H groups and the OAc^-, followed by proton transfer to form a $\{[Ru(bpy)_2(Hbbim)]\cdot HOAc\}$ association. This was further confirmed by an ESI-MS experiment, in which two clear clusters of isotopic peaks centered at $m/z = 647.1$ and 709.1 assigned to $[Ru(bpy)_2(Hbbim)]^+$ and $[\{Ru(bpy)_2(Hbbim)\cdot HOAc\}]^+$, respectively, were observed by the modulation of voltage (see Figure S4 in the Supporting Information).

(36) Rampi, M. A.; Indelli, M. T.; Scandola, F.; Pina, F.; Parola, A. J. *Inorg. Chem.* **1996**, *35*, 3355.

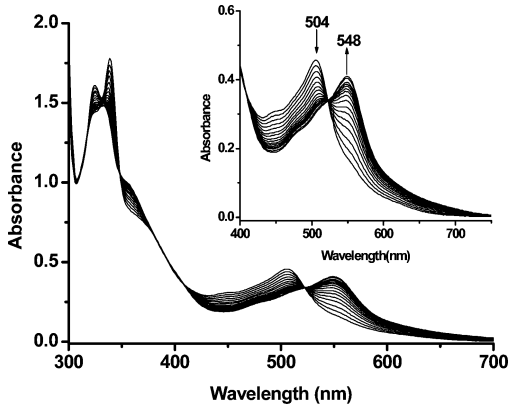

Figure 6. UV−vis titration of **1** in MeCN solution (5×10^{-5} M) upon addition of Bu_4NOAc (1 to 5 equivalents). Insert: Absorption spectra in the range of 400−750 nm.

The equilibrium $[Ru(bpy)_2(H_2bbim)]^{2+} + OAc^- \rightleftarrows \{[Ru(bpy)_2(Hbbim)]\cdot HOAc\}$ is established, and its binding constant can be given by $\log K_1 = 5.06$ via a fitting of the experimental data of OAc^- anion to the changes of absorbance.[37]

Second, when more than 1 equiv of $[Bu_4N]OAc$ was added to the solution of **1**, the color of the solution turned from orange brown to violet (see Figure 2). The band at 504 nm decreases, and a new band grows at 548 nm; these stop at 2 equiv of OAc^- anion addition. Three isosbestic points at 349, 406, and 522 nm were observed in the titration profile, indicating that only two species coexist at the equilibrium (Figure 6). The profiles of the absorbances at 504 (decreasing) and 548 nm (increasing) demonstrated a 1:1 stoichiometry interaction. To assign the band at 548 nm, the double-deprotonated complex $[Ru(bpy)_2(bbim)]$ **3** was synthesized by addition of NaOH. The spectra show they are the same species (see Figure S5 in the Supporting Information). Therefore, the equilibrium $\{[Ru(bpy)_2(Hbbim)]\cdot HOAc\} + OAc^- \rightleftarrows [Ru(bpy)_2(bbim)] + 2HOAc$ is established, and its binding constant can be given by $\log K_2 = 5.79$ via a fitting of the experimental data of OAc^- anion.[37] This observation results from the formation of the monodeprotonated $\{[Ru(bpy)_2(Hbbim)]\cdot HOAc\}$ association in the first stage with a low OAc^- concentration, followed by double-deprotonation in the presence of a high OAc^- concentration to produce the neutral species **3** and a stable ($CH_3COOH\cdots HOOCCH_3$) dimer in solution.[38]

The deprotonation processes in **1** are much different from the previous observation of the interaction between $[Ru(bpy)_2(H_2biim)](PF_6)_2$ and OAc^- anion, in which only monodeprotonation takes place upon addition of 2 equiv of OAc^- anion to the solution of $[Ru(bpy)_2(H_2biim)](PF_6)_2$.[18] These may be attributed to the larger pK_{a2} value of $[Ru(bpy)_2(H_2biim)](PF_6)_2$ (12.0, where the pK_{a2} value of **1** is 10).[26,27]

The strong interaction between metalloreceptor **1** and OAc^- anion is also confirmed by ^1H NMR spectroscopy in

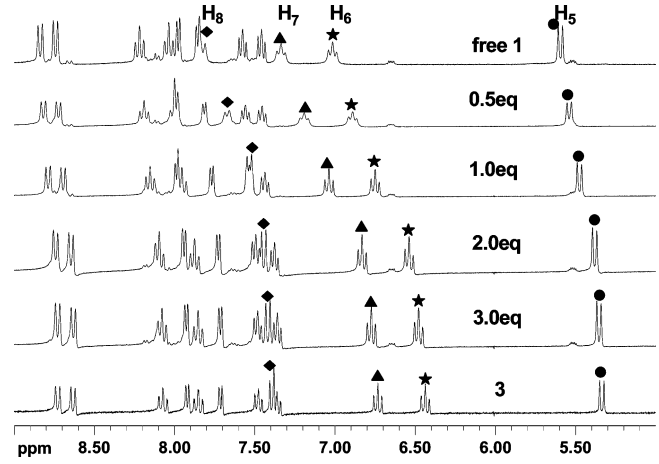

Figure 7. ^1H NMR spectra of **3** and the titration of **1** (7.5×10^{-3} M) in DMSO-d_6 with OAc^- anion.

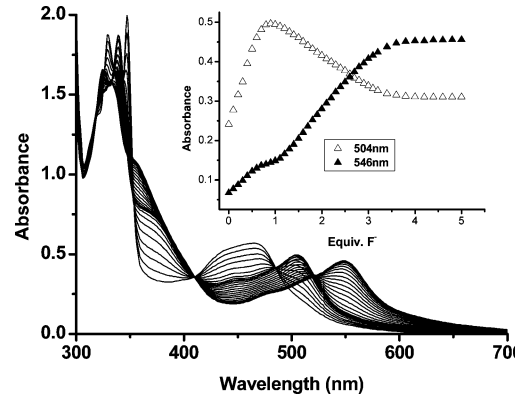

Figure 8. UV−vis titration of **1** in MeCN solution (5×10^{-5} M) upon addition of Bu_4NF (0−5 equiv). Insert: Absorbances at 504 and 546 nm versus equiv of F^- anion.

DMSO-d_6 solution where **1** has a higher solubility. A 7.5×10^{-3} M solution of **1** in DMSO-d_6 was titrated with OAc^- anion up to 3 equivalents. As shown in Figure 7, though the signals of N−H protons in the H_2bbim ligand are unobserved in the present case, the chemical shifts of C−H protons of H_2bbim (H_5, H_6, H_7 and H_8) are very sensitive upon addition of OAc^- anion. Upon addition of OAc^- anion, the chemical shifts of H_5, H_6, H_7, and H_8 are progressively upfield shifted and stop at 2 equiv of addition because of charge delocalization on the entire conjugated system with the deprotonation of N−H group. The final displacements for H_5, H_6, H_7, and H_8 are 0.25, 0.58, 0.56 and 0.42 ppm, respectively. The upfield signal is assigned to H_5 because it is closer to the bpy ligand and suffered from the ring current effect of bpy.[28,39]

Similar trends of spectral changes have been observed upon addition of F^- anion to the solution of **1** (see Figures 1, 2, S2, S3, and S5−S7). Figure 8 displays the complete family of spectra displacement and the absorption intensity variety of the bands at 504 (first increasing and then decreasing) and 546 nm (increasing) during the titration of a 5×10^{-5} M solution of **1** in MeCN with $[Bu_4N]F$. This

(37) Liu, Y.; Han, B.-H.; Chen, Y-T. *J. Phys. Chem. B* **2002**, *106*, 4678.
(38) (a) Boiocchi, M.; Del Boca, L.; Esteban-Gómez, D.; Fabbrizzi, L.; Licchelli, M.; Monzani, E. *Chem.—Eur. J.* **2005**, *11*, 3097. (b) Lin, T.-P.; Chen, C.-Y.; Wen, Y.-S.; Sun, S.-S. *Inorg. Chem.* **2007**, *46*, 9201.
(39) (a) Hitchcock, P. B.; Seddon, K. R.; Turp, J. E.; Yousif, Y. Z.; Zora, J. A.; Constable, E. C.; Wernberg, O. *J. Chem. Soc., Dalton. Trans.* **1988**, 1837. (b) Ye, B.-H.; Ji, L.-N.; Xue, F.; Mak, T. C. W. *Transition Met. Chem.* **1999**, *24*, 8.

observation suggests that the monodeprotonated [Ru(bpy)$_2$(Hbbim)] formed first, followed by double-deprotonation to produce the neutral species **3** and a stable HF_2^- anion in solution. The difference is that an additional 2 equiv of F^- is needed to trap the second proton from **1**, whereas only another 1 equiv of OAc^- anion is necessary. This may be considered because one more equiv of F^- anion is needed to form the highly stable HF_2^- dimer,[40] which was further confirmed by ^{1}H NMR titration experiments featuring a triplet characteristic peak at 16.1 ppm in MeCN-d_3 solution. The binding constant of **1** and F^- anion can be given by log $K_1 = 5.28$ via a fitting of the experimental data of F^- anion,[37] which is comparable to that of **1** and OAc^- anion (log $K_1 = 5.06$). The constant of K_2 is related to the second acidity constant of **1** and the formation constant of HF_2^-. On the other hand, the titration profile is much different from the observation of the interaction of [Ru(bpy)$_2$(H$_2$biim)](PF$_6$)$_2$ and F^- anion,[18] in which 8 equiv of F^- anion is needed to trap the N−H protons from Ru(II)-H$_2$biim. This may be attributed to an especially high value of pKa_2 (12) of [Ru(bpy)$_2$(H$_2$biim)](PF$_6$)$_2$.[26,27] In general, **1** exhibits high sensitivity to OAc^- and F^- anions but lacks good selectivity to explicitly differentiate these two anions.

Proton Transfer between Ru(II)-bbim and Carboxylic acids. The absorption and NMR experiments all show that **1** is double-deprotonated to form the neutral species [Ru(bpy)$_2$(bbim)] upon addition of 2 equiv of OAc^- anion. This should be related to the acidity of N−H group in given receptor and the basicity of anion. It is known that OAc^- anion behaves as a strong base with p$K_a = 21.6$ in MeCN.[41] To further examine this observation, the double-deprotonated species **3** was synthesized and used to observe the interaction with carboxylic acids. The neutral species **3** was double-protonated when 2 equiv trifluoroacetic acid (p$K_a = 13.0$ in MeCN)[42] was introduced to the solution of **3** in MeCN because of the Brönsted acid−base reaction equilibrium. The band at 548 nm blue-shifted to 465 nm (see Figures 9 and S9), and the original, violet solution turned to yellow. These stimulated us to observe the proton transfer between the Ru(II)-H$_2$bbim and other carboxylic acid with different pK_a values. Surprisingly, when 2 equiv of trichloroacetic acid was employed in place of CF_3CO_2H, the peak at 548 nm was displaced to 504 nm (Figure 9), demonstrating that **3** was monoprotonated. This may be attributed to the formation of 2-fold hydrogen bonds between **1** and $CCl_3CO_2^-$ because they are geometrically matched and form

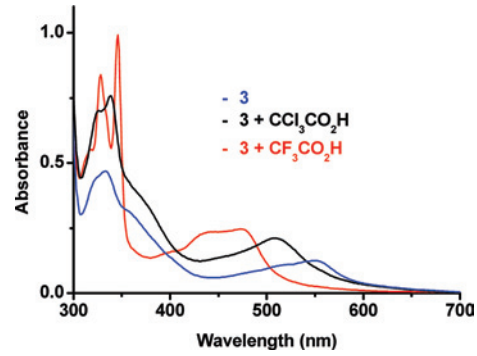

Figure 9. UV−vis spectra of [Ru(bpy)$_2$(bbim)]·CH$_3$OH·H$_2$O (**3**, blue), **3** plus 2 equiv of CCl_3CO_2H (black), and **3** plus 2 equiv of CF_3CO_2H (red) in MeCN solution.

complementary linear "Y-type" hydrogen bonds.[43] The formation of robust hydrogen bonds between **1** and $CCl_3CO_2^-$ anion assists the proton transfer (PT); finally, the H$_2$bbim ligand is monodeprontonated (Scheme S2 in the Supporting Information). From the above observations, a conclusion can be drawn out that proton transfer is not only determined by the basicity of anion but also related to the strength of hydrogen bonding interaction.

Crystal Structures of 2 and 4. To elucidate the hydrogen bonding interaction between Ru(II)-H$_2$bbim and carboxylate groups in the solid state, crystal structures of **2** and **4** were measured. As expected, each Ru(II) ion is coordinated by two bpy and one H$_2$bbim (or Hbbim) ligands in a distorted octahedral coordination. The structural parameters of the coordination sphere and the ligands are all in normal.[18,19,22,44] The peripheral N−H group and nitrogen atom form 2-fold, complementary hydrogen bonds with a carboxylic acid (see Figures 10). The hydrogen bonding distances of N7···O1A =2.640(7) and N8···O2A = 2.679(6) Å for **2**, N7···O3A = 2.630(5),and N8···O4A = 2.781(5) Å for **4**, and the average angle of N−H···O = 173° are all in the range of strong hydrogen bonding.[30,45–47] The bond distance C70A−O1A = 1.230(8) Å is slightly shorter than that of C70A−O2A = 1.271(8) Å in **2**. A similar case is also observed in **4**, in which the C38A−O4A = 1.209(8) Å is shorter than C38A−O3A = 1.237(8) Å. These observations all indicate that they are asymmetric interaction. Although exact assign-

(40) (a) Shenderovich, I. G.; Tolstoy, P. M.; Golubev, N. S.; Smirnov, S. N.; Denisov, G. S.; Limbach, H.-H. *J. Am. Chem. Soc.* **2003**, *125*, 11710. (b) Boiocchi, M.; Boca, L. D.; Esteban-Gómez, D.; Fabbrizzi, L.; Licchelli, M.; Monzani, E. *J. Am. Chem. Soc.* **2004**, *126*, 16507. (c) Esteban-Gómez, D.; Fabbrizzi, L.; Licchelli, M. *J. Org. Chem.* **2005**, *70*, 5717. (d) Kang, S. O.; Powell, D.; Day, V. W.; Bowman-James, K. *Angew. Chem., Int. Ed.* **2006**, *45*, 1921. (e) Wu, Y.; Peng, X.; Fan, J.; Gao, S.; Tian, M.; Zhao, J.; Sun, S. *J. Org. Chem.* **2007**, *72*, 62.
(41) Bartnicka, H.; Bojanowska, I,; Kalinowski, M. K. *Aust. J. Chem.* **1991**, *44*, 1077.
(42) Pawlak, Z.; Tusk, M.; Kuna, S.; Strohbusch, F.; Fox, M. F. *J. Chem. Soc., Faraday Trans. 1* **1984**, 1757.
(43) (a) Smith, P. J.; Reddington, M. V.; Wilcox, C. S. *Tetrahedron Lett.* **1992**, *41*, 6085. (b) Fan, E.; van Arman, S. A.; Kincaid, S.; Hamilton, A. D. *J. Am. Chem. Soc.* **1993**, *115*, 369.
(44) (a) Majumdar, P.; Kamar, K. K.; Castiñeiras, A.; Goswami, S. *Chem. Commun.* **2001**, 1292. (b) Benkstein, K. D.; Stern, C. L.; Splan, K. E.; Johnson, R. C.; Walters, K. A.; Venhelmont, F. W. M.; Hupp, J. T. *Eur. J. Inorg. Chem.* **2002**, 2818.
(45) (a) Ye, B.-H.; Xue, F.; Xue, G.-Q.; Ji, L.-N.; Mak, T. C. W *Polyhedron* **1999**, *18*, 1785. (b) Ye, B.-H.; Ding, B.-B.; Weng, Y.-Q.; Chen, X.-M. *Inorg. Chem.* **2004**, *43*, 6866. (c) Ye, B.-H.; Ding, B.-B.; Weng, Y.-Q.; Chen, X.-M. *Cryst. Growth Des.* **2005**, *5*, 801. (d) Ding, B.-B.; Weng, Y.-Q.; Mao, Z.-W.; Lam, C.-K.; Chen, X.-M.; Ye, B.-H. *Inorg. Chem.* **2005**, *44*, 8836. (e) Ding, B.-B.; Weng, Y.-Q.; Cui, Y.; Chen, X.-M.; Ye, B.-H. *Supramol. Chem.* **2005**, *17*, 475.
(46) (a) Tadokoro, M.; Fukui, S.; Kitajima, T.; Nagao, Y.; Ishimaru, S.; Kitagawa, H.; Isobe, K.; Nakasuji, K. *Chem. Commun.* **2006**, 1274. (b) Ghosh, A. K.; Jana, A. D.; Ghoshal, D.; Mostafa, G.; Chaudhuri, N. R. *Cryst. Growth Des.* **2006**, *6*, 701. (c) Sang, R.-L.; Xu, L. *Inorg. Chim. Acta* **2006**, *359*, 525.
(47) (a) Atencio, R.; Chacon, M.; Gonzalez, T.; Briceno, A.; Agrifoglio, G.; Sierraalta, A. *Dalton Trans.* **2004**, 505. (b) Larsson, K.; Öhrström, L. *CrystEngComm* **2004**, *6*, 354.

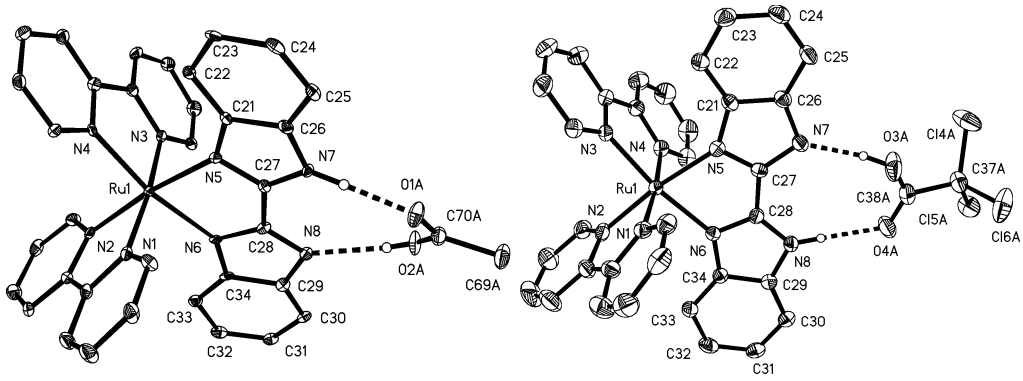

Figure 10. Molecular structure of complexes **2** (left) and **4** (right); some hydrogen atoms, water molecules, and the Cl^- anion are omitted for clarity. Symmetry code: A x, $-1+y$, z for **2**; $1-x$, $1-y$, $-z$ for **4**.

ment of the hydrogen atom between the nitrogen and oxygen is impossible because the accurate position of hydrogen atom cannot be located via X-ray diffraction, the reasonable case is the H_2bbim ligand is monodeprotonated. The complementary topology of the H_2bbim segment and the carboxylate anions ($R_2^2(9)$ synthon) allows a more efficient interaction between two parts leading to proton transfer from one NH group of the H_2bbim ligand to the carboxylate.[48] These are consistent with the observated result of absorption and ESI-Ms spectra.

Complex **2** consists of two $[Ru(bpy)_2(Hbbim)]$ cations, two Cl^-, three acetic acid, and 12 water molecules (see Experimental Section). Each $[Ru(bpy)_2(Hbbim)]^{2+}$ cation attaches an acetic acid via 2-fold hydrogen bonds, then further connects to each other via the formation of hydrogen bonds with the water molecules and the acetic acid, resulting in a 1D chiral chain ($\Lambda-\Lambda-\Lambda$ or $\Delta-\Delta-\Delta$) as shown in Figure 11. Two chiral chains connect each other via the water molecules (O7W···O1W = 2.791(8), O5W···O7W = 2.731(9), and O3W···O1W = 2.824(9) Å) into a double racemic chain along the *c*-axis. These double chains pack each other through strong $\pi-\pi$ interaction (3.35 and 3.37 Å) between the H_2bbim ligands into a 2D layer on the *bc* plane as shown in Figure 12.

Crystal Structures of 3. To compare the changes of the structural parameters between the monodeprotonated and bideprotonated ligand of H_2bbim, the double-deprotonated species **3** was synthesized and measured by X-ray single crystal determination. It consists of one $[Ru(bpy)_2(bbim)]$ neutral molecule, one methanol, and one water molecules. As expected, Ru(II) ion is coordinated by two bpy and one bbim ligands in a distorted octahedral coordination (Table 2). The deprotonated ligand bbim behaves as a hydrogen bonded acceptor from the methanol solvent (O1···N7 = 2.805(6) Å) and the lattice−water molecule (O1w···N8 = 2.979(7) Å) as shown in Figure 13. The distances of Ru(II)−N(bpy) (2.032(2)−2.047(2) Å) are slightly shorter than those of Ru(II)−N(bbim) (2.084(3)−2.087(4) Å). These are agreement with the observations in compounds **2** (Ru(II)−N(bpy) = 2.042(5)−2.064(5) Å and Ru(II)−N(Hbbim) = 2.092(5)−2.103(5) Å), **4** (Ru(II)−N(bpy) = 2.040(4)−2.054(3) Å and Ru(II)−N(Hbbim) = 2.094(4)−2.103(4) Å),

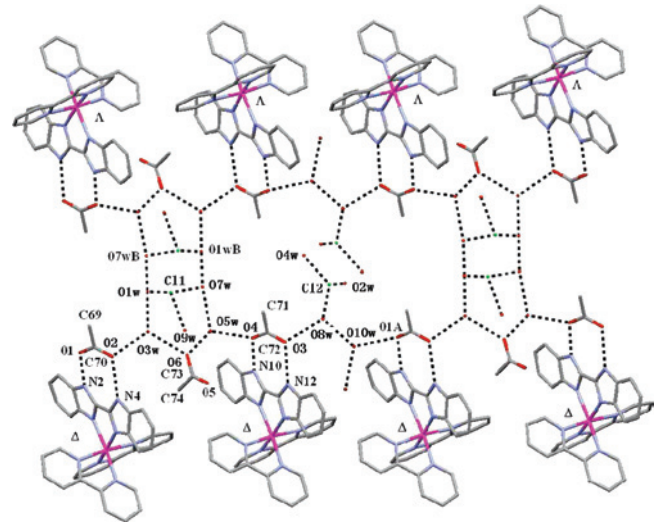

Figure 11. View of the hydrogen bonding chain of **2** in the solid state. Selected hydrogen bonding distances (Å): Cl2···O2W = 3.212(8), Cl2···O4W = 3.176(6), Cl2···O8W = 3.158(9), Cl1···O5W = 3.017(7), Cl1···O7W = 3.246(7), Cl1···O9W = 3.107(2), O1···O10W = 2.722(8), O1W···O10W = 2.718(8), O8W···O10W = 2.710(9), O8W···O3 = 2.730(7), O6W···O4 = 2.650(7), O5W···O6W = 2.827(8), O5W···O7W = 2.731(9), O6···O6W = 2.597(8), O6···O3W = 2.845(8), O3W···OW = 2.824(9), O3W···O2 = 2.684(7). Symmetry code: A x, y, $1+z$; B $-x$, $-y$, $-z$.

$[Ru(tbpy)_2(bbim)]$ (Ru(II)−N(tbpy) = 2.046(3)−2.050(3) Å and Ru(II)−N(bbim) = 2.101(3) Å),[19] and $Ru(bpy)_2(H_2bbim)](CF_3SO_3)_2$ (Ru(II)−N(bpy) = 2.046(3)−2.065(3) Å and Ru(II)−N(H_2bbim) = 2.101(3) Å]).[49] The bite angles of N−Ru−N are 77.4(1)−79.0(1)° are also comparable to those observed in complexes **2** (78.0(2)−79.7(2)°), **4** (77.8(1)−79.0(1)°), $[Ru(tbpy)_2(bbim)]$ (77.8(3)−78.7(3)°),[19] and $[Ru(bpy)_2(H_2bbim)](CF_3SO_3)_2$ (77.7(1)−78.9(1)°),[49] indicating that no significant structural changes in the primary coordination sphere are induced by deprotonation. However, some differences in the coordinated Hbbim (bbim) ligand are observed by careful comparison their geometries. First, the bond lengths C27−N7 = 1.341(5) Å and C28−N8 = 1.336(5) Å are shorter than those of C27−N5 = 1.353(5) Å and C28−N6 = 1.356(5) Å. However, the reverse cases were observed in $[Ru(bpy)_2(H_2bbim)](CF_3SO_3)_2$,[49] **2**, and **4**, (see

(48) Steiner, T. *Angew. Chem., Int. Ed.* **2002**, *41*, 48.

(49) Rau, S.; Ruben, M.; Buttner, T.; Temme, C.; Dautz, S.; Gorls, H.; Rudolph, M.; Walther, D.; Brodkorb, A.; Duati, M.; O'Connor, C.; Vos, J. G. *J. Chem. Soc., Dalton Trans.* **2000**, 3649.

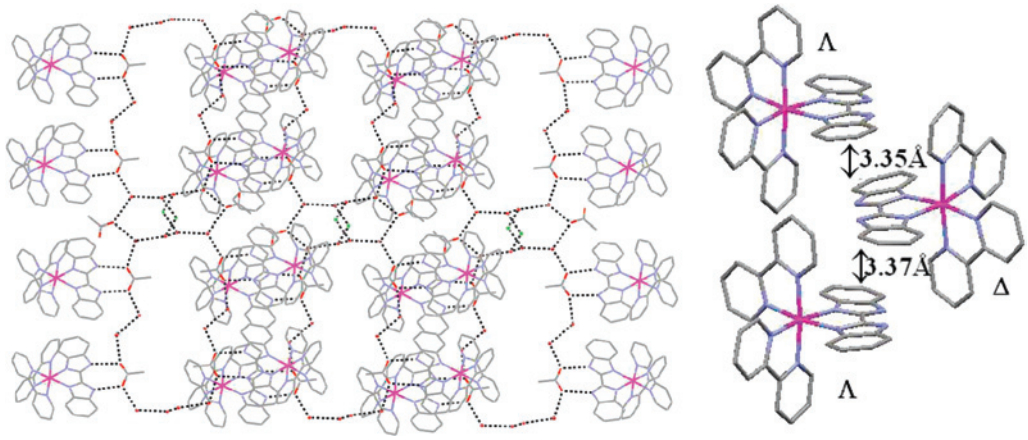

Figure 12. 2D structure of **2** on the *bc* plane (left) and $\pi-\pi$ packing on *c*-axis (right).

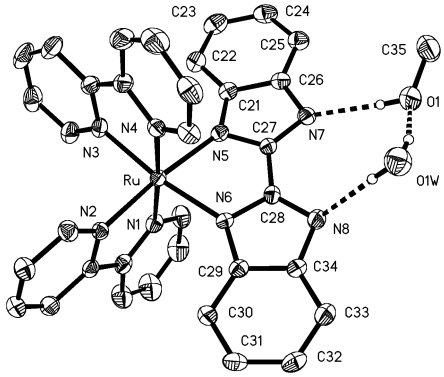

Figure 13. Molecular structure of complex **3**; some of the hydrogen atoms are omitted for clarity.

Table 2). Second, the angles N5−C27−N7 = 116.5(2)° and N6−C28−N8 = 116.4(2)° for **3** are larger than those of **2** (113.0(6) and 115.8(5)°), **4** (113.8(4) and 112.7(4)°), and $[Ru(bpy)_2(H_2bbim)](CF_3SO_3)_2$ (113.2(3)°).[49] In addition, the angles C21−N5−C27 = 103.8(2)°, C27−N7−C26 = 102.5(3)°, C28−N6−C34 = 103.9(2)°, C28−N8−C34 = 102.9(3)° for **3** are smaller than those of **2** (104.9(5)°, 106.9(5)°, 105.1(5)°, and 104.6(5)°) and **4** (105.7(4)°, 105.3(3)°, 105.8(3)°, and 107.3(4)°). Whereas the angles N7−C26−C21 = 109.7(2)° and N8−C34−C29 = 109.2(2)° are larger than the corresponding angles in **2** (106.4(5)° and 107.1(5)°) and **4** (107.4(4)° and 106.0(4)°). All these indicate that the deprotonation induces the electron delocalization and redistribution.

Conclusion

In conclusion, we have developed an anion receptor **1** based on Ru(II)-bpy moiety as a chromophore and the H_2bbim ligand as an anion binding site. The study presents that **1** interacts with the Cl^-, Br^-, I^-, NO_3^-, HSO_4^-, and $H_2PO_4^-$ anions via the formation of hydrogen bonds. Whereas **1** undergoes a stepwise process with the addition of F^- and OAc^- anions, formation of the monodeprotonated complex $[Ru(bpy)_2(Hbbim)]$ with a low anion concentration, followed by the double-deprotonated complex $[Ru(bpy)_2(bbim)]$ in the presence of a high anion concentration. These stepwise processes concomitant with the changes of vivid colors from yellow to orange brown, then, to violet can be used for probing the F^- and OAc^- anions by naked eye. The interactions are not only determined by the basicity of the anion but also related to the strength of hydrogen bonding.

Acknowledgment. This work was supported by the NSF of China (No. 20771104) and Guangdong Province (No. 20623086), the Doctoral Programs Foundation of Ministry of Education of China (No. 20070558009), and the NSF for Fostering Talents of Basic Science (No. J0730420).

Supporting Information Available: TG for **2**, spectra of **1** in the present of F^-, OAc^-, and NaOH, and X-ray crystallographic file in CIF format for the structure determination of **2**, **3** and **4**. This material is available free of charge via the Internet at http://pubs.acs.org.

IC702050B